Upregulation of CYR61 by TGF-β and YAP signaling exerts a counter-suppression of hepatocellular carcinoma

Cheng Zhang[1,2,‡], Wenjing Wei[1,‡], Shuo Tu[1], Bo Liang[3], Chun Li[2], Yining Li[1], Weicheng Luo[1], Yiqing Wu[1], Xiaohui Dai[1], Yi Wang[1], Lijuan Zheng[1], Liang Hao[3], Chunbo Zhang[4], Zhijun Luo[5], Ye-Guang Chen[1,6], and Xiaohua Yan[1,2,*]

From the [1]The MOE Basic Research and Innovation Center for the Targeted Therapeutics of Solid Tumors, School of Basic Medicine, [2]The First Affiliated Hospital, [3]The Second Affiliated Hospital, [4]School of Pharmacy, and [5]Queen Mary School, Jiangxi Medical College, Nanchang University, Nanchang, China; [6]School of Life Sciences, Tsinghua University, Beijing, China

Reviewed by members of the JBC Editorial Board. Edited by Eric Fearon

Transforming growth factor-β (TGF-β) and Hippo signaling are two critical pathways engaged in cancer progression by regulating both oncogenes and tumor suppressors, yet how the two pathways coordinately exert their functions in the development of hepatocellular carcinoma (HCC) remains elusive. In this study, we firstly conducted an integrated analysis of public liver cancer databases and our experimental TGF-β target genes, identifying CYR61 as a pivotal candidate gene relating to HCC development. The expression of CYR61 is downregulated in clinical HCC tissues and cell lines than that in the normal counterparts. Evidence revealed that CYR61 is a direct target gene of TGF-β in liver cancer cells. In addition, TGF-β-stimulated Smad2/3 and the Hippo pathway downstream effectors YAP and TEAD4 can form a protein complex on the promoter of CYR61, thereby activating the promoter activity and stimulating CYR61 gene transcription in a collaborative manner. Functionally, depletion of CYR61 enhanced TGF-β- or YAP-mediated growth and migration of liver cancer cells. Consistently, ectopic expression of CYR61 was capable of impeding TGF-β- or YAP-induced malignant transformation of HCC cells *in vitro* and attenuating HCC xenograft growth in nude mice. Finally, transcriptomic analysis indicates that CYR61 can elicit an antitumor program in liver cancer cells. Together, these results add new evidence for the crosstalk between TGF-β and Hippo signaling and unveil an important tumor suppressor function of CYR61 in liver cancer.

As the major form of primary liver cancers, hepatocellular carcinoma (HCC) is one of the most lethal cancer types worldwide (1). The homeostasis of the adult liver is regulated by both transforming growth factor-β (TGF-β) and Hippo signaling pathways, aberration of which contributes to the development of various liver diseases, including liver cancer (2–6). TGF-β is highly expressed in advanced liver cancers and promotes the proliferation, migration, and invasion of cancer cells, among other tumor-promoting actions (6–8). Upon TGF-β stimulation, R-Smad proteins (Smad2/3) and the common Smad (Co-Smad, Smad4) form a protein complex and accumulate in the nucleus, where they regulate gene transcription by binding to DNA directly and associating with other transcriptional regulators (9–11).

The Hippo pathway exerts an inhibitory role in liver cancer development by inactivating the downstream transcriptional coactivators YAP and TAZ, which have been frequently found to be hyperactivated or overexpressed in liver cancer (3, 12). At the core of the Hippo pathway are MST1/2 and LATS1/2 serine/threonine kinases (13, 14). Once activated by MST1/2, LATS1/2 phosphorylates and inactivates YAP and TAZ. The Hippo kinase cascade is shut off in response to growth factors, cell polarity changes or mechanic cues, enabling activation of YAP/TAZ and their association with TEAD family transcription factors (TEADs 1-4) (13, 14).

As the downstream transcriptional regulators of the TGF-β and Hippo pathways, Smads and YAP/TAZ/TEADs, respectively, exert diverse biological functions in liver cancer *via* regulating gene expression (2, 3, 5, 6, 12). Indeed, previous studies have revealed that a large array of Smads-regulated effectors can mediate the protumor functions of TGF-β in liver cancer, such as LXRα, SNAI1, CTGF, and AXL (7, 15–18). Intriguingly, CTGF and AXL have also been demonstrated to be transcriptionally upregulated upon Hippo signaling inactivation and mediate the oncogenic actions of YAP and/or TAZ in liver cancer (19, 20). Smads and YAP/TAZ/TEADs have been shown to play important roles in embryonic development, stem cell fate determination and cancer progression *via* convergence on gene transcriptional regulation (21–24). For instance, TGF-β and Hippo signaling can orchestrate a Smad2/3-YAP-TEAD-p300 complex on the promoter of CTGF, regulating its expression and malignant mesothelioma progression (25). However, how TGF-β-activated Smads interplay with YAP/TEADs in liver cancer is not well understood.

Although both CYR61 (CCN1) and CTGF (CCN2) are secreted extracellular matrix proteins that belong to the same matricellular protein family, the functions of CYR61 in cancer seem to be context-dependent (26). While promoting the development of breast cancer, colorectal cancer, pancreatic cancer, and glioma, CYR61 has been evidenced to exert an inhibitory role in liver cancer, non–small cell lung cancer and

---

melanoma (27–29). How CYR61 is transcriptionally controlled in liver cancer and how it suppresses HCC development are yet to be elucidated.

In this study, CYR61 was identified as one of the key candidates dysregulated in HCC. We found that TGF-β-activated Smad2/3 concerted with YAP/TEAD4 to regulate the promoter activity and transcription of CYR61 in liver cancer cells. CYR61 can ameliorate TGF-β- and YAP activation-induced malignant transformation of liver cancer cells *in vitro* and HCC xenograft growth *in vivo*. These results shed new light on the tumor-suppressive function of CYR61 in liver cancer, and highlight the interplay of TGF-β and Hippo signaling pathways in controlling CYR61 gene transcription.

Results

Identification of CYR61 as a candidate gene regulating HCC

To gain insight into the pathogenesis of HCC, we analyzed differentially expressed genes (DEGs) between HCC tissues and normal liver tissues from public databases. First, mining of 5 Gene Expression Omnibus (GEO) liver cancer datasets revealed 1497 upregulated genes and 736 downregulated genes in HCC tissues when compared with normal tissues (Fig. S1 and Table S1). Then, we screened DEGs by comparing the four tumor, node, metastasis (TNM) stages (stages i-iv) of HCC samples with normal liver samples in The Cancer Genome Atlas (TCGA) liver hepatocellular carcinoma (LIHC) database (Figs. S1 and S2). A total of 559 upregulated genes and 214 downregulated genes were identified. Two hundred ninteen genes displayed similar expressional changes in both the TCGA and GEO databases, as shown in the Venn plot map (Fig. 1A) and clustered heatmap results (Fig. 1B).

To identify the context-dependent effectors of TGF-β in liver cancer, three HCC cell lines, *i.e.*, MHCC97H, MHCC97L, and HCCLM3, were treated with recombinant TGF-β1 protein for 4 h, followed by transcriptome sequencing (RNA-Seq) analysis. As a result, the expressions of 463 genes were found to be similarly changed upon TGF-β stimulation in the three
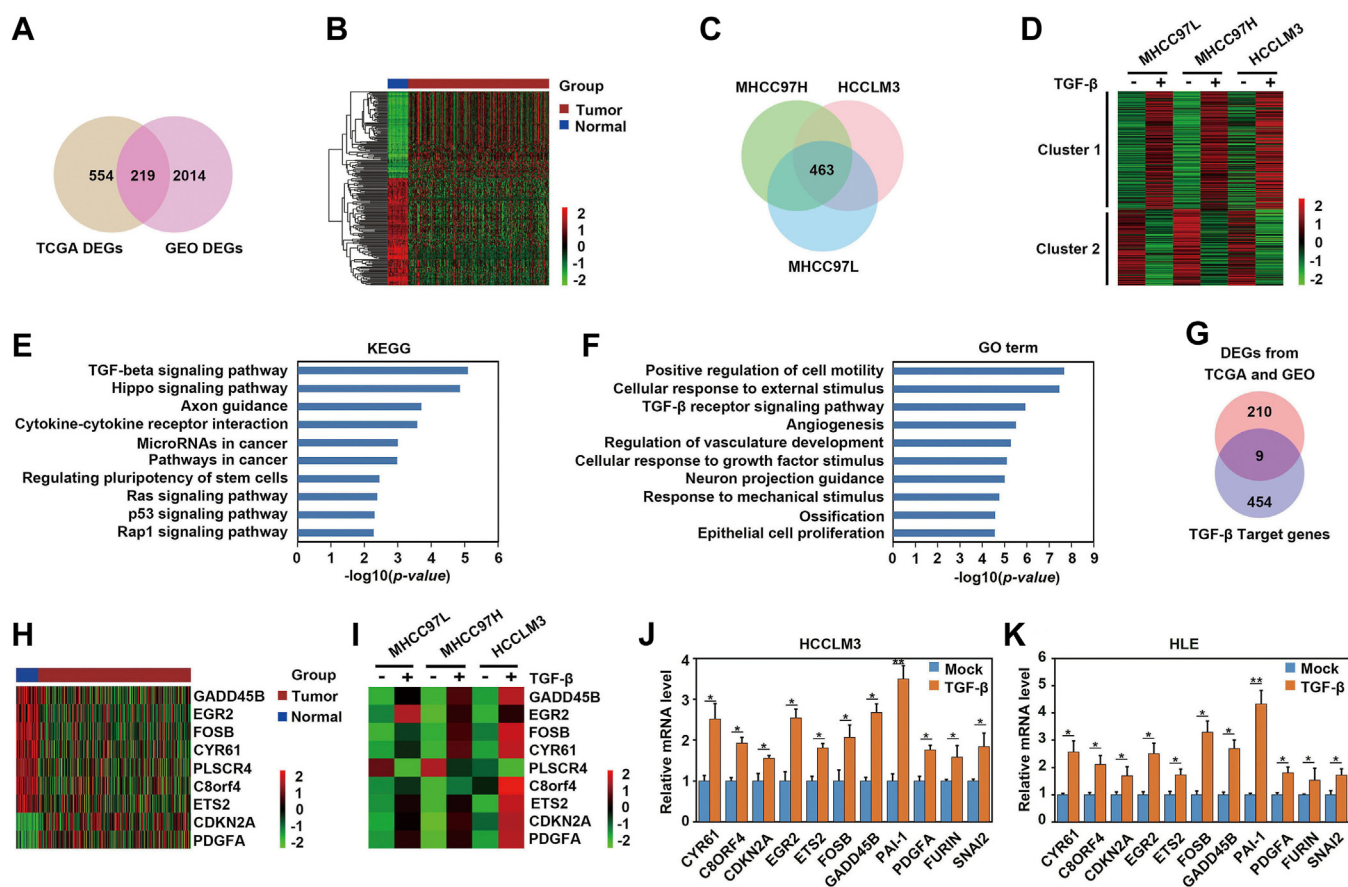
Figure 1. Identification of CYR61 as a key candidate gene relating to HCC development. *A* and *B*, venn diagram (*A*) and heatmap classification (*B*) showing the overlapping 219 differentially expressed genes (DEGs) whose expression levels were significantly changed between HCC tissues and normal liver tissues in both TCGA and GEO liver cancer databases. Details of the analyses were described in the Experimental procedures. Color-encoded relative gene expression levels are expressed in log2 scale. *C* and *D*, Venn diagram (*C*) and heatmap classification (*D*) displaying the 463 overlapping DEGs whose expressions were altered upon TGF-β1 treatment in MHCC97H, MHCC97L, and HCCLM3 cell lines. Cancer cells were stimulated with or without 2.5 ng/ml of recombinant TGF-β1 protein for 4 h before being subjected to total RNA isolation and transcriptome sequencing (RNA-Seq). *E* and *F*, KEGG pathway enrichment (*E*) and GO term analysis (*F*) of TGF-β target genes. *G*, venn diagram indicating the nine common genes between database mining results and experimental TGF-β target gene dataset. *H* and *I*, heatmaps demonstrating the expression of the above nine shared genes in TCGA database (*H*) and in liver cancer cells upon TGF-β stimulation (*I*), respectively. *J* and *K*, HCCLM3 (*J*) and HLE (*K*) cells were stimulated with or without 2.5 ng/ml of TGF-β1 for 4 h, followed by total RNA extraction and quantitative PCR analysis. *$p < 0.05$, **$p < 0.01$ and ***$p < 0.001$ were calculated using two-tailed student *t* test (*J* and *K*), and data were shown as mean ± SD. DEGs, differentially expressed genes; GEO, Gene Expression Omnibus; GO, gene ontology; HCC, hepatocellular carcinoma; KEGG, Kyoto Encyclopedia of Genes and Genomes; TCGA, The Cancer Genome Atlas; TGF-β, transforming growth factor-β.

cell lines (Fig. 1, *C* and *D*). Among these genes, 283 (cluster 1) were transcriptionally activated whereas 180 (cluster 2) were repressed. Gene ontology term and Kyoto Encyclopedia of Genes and Genomes enrichment analyses revealed that the TGF-β-regulated genes were closely related to cell motility, cellular response to external stimulus, TGF-β signaling and Hippo signaling, among others (Fig. 1, *E* and *F*).

Intriguingly, by comparison of the public database mining results and our experimental TGF-β target genes, nine genes were identified as potential candidates that may regulate liver cancer development, including CYR61 (Fig. 1, *G–I*). These genes were experimentally verified to be transcriptionally regulated by TGF-β in different HCC cell lines (Figs. 1, *J* and *K*, and S3).

Downregulation of CYR61 in liver cancer predicts bad outcomes in patients

Among the nine candidate genes that may regulate HCC development, CYR61 is of particular interest as it acts as an injury-responsive gene in the liver and plays a protective role against the development of hepatic fibrosis and liver cancer, although the underlying molecular mechanisms and clinical relevance still need in-depth investigations (29–33). Therefore, we explored the expression of CYR61 in human HCC patients. Both the mRNA and protein expression levels of CYR61 were significantly downregulated in most clinical tumor tissues than that in the normal counterparts (Fig. 2, *A* and *B*). In addition, mining of the TCGA-LIHC database revealed a reduced CYR61 expression in HCC tissues compared with the normal liver tissues (Fig. 2*C*), in tumor samples than their paired normal liver tissues (Fig. 2*D*), or in all the four tumor, node, metastasis stages of HCC tissues than in normal tissues (Fig. 2*E*). Importantly, the expression level of CYR61 in liver cancer was positively correlated with survival time in human patients (Fig. 2*F*). These results were also supported by mining of the ICGC-LIRI-JP database (Fig. 2, *G–J*). In addition, the expression of CYR61 was also lower in HCC cell lines than that in a normal hepatocyte line LO2 (Fig. 2, *K* and *L*). Together, the above results demonstrate that CYR61 is intimately linked to TGF-β signaling and HCC development.

CYR61 is a direct target gene of TGF-β in liver cancer cells

To validate the transcriptional regulation of CYR61 by TGF-β, we treated four different liver cancer cell lines with TGF-β1. As shown in Figure 3, *A* and *B*, TGF-β not only induced the expression of plasminogen activator inhibitor-1 (PAI-1), a hallmark of TGF-β actions in various contexts, but also increased that of CYR61 at both the mRNA and protein levels. In accordance with this, treatment with SB431542, a small chemical inhibitor of TGF-β type I receptor, apparently decreased the expression of CYR61 in HCC cells (Fig. 3*C*). Moreover, knockdown of Smad2, Smad3, or Smad4 significantly reduced TGF-β-elicited CYR61 expression in both HLE and HCCLM3 cells, indicating the canonical Smad pathway is involved (Fig. 3*D*).

Next, we assessed whether TGF-β and Smads regulate the promoter activity of CYR61 gene. To this end, different CYR61 gene promoter fragments were cloned to construct a series of promoter luciferase reporters, designated as CYR61-pro-luciferase (Fig. 3*E*). As shown in Figure 3*F*, the promoter DNA fragments that contain the −222 to −118 bp upstream of the transcription start site (TSS) of CYR61 were well responsive to TGF-β. A subsequent reporter assay using the CYR61-pro-luciferase construct (−222/+15) showed that ectopically expressed Smad2 or Smad3, with or without Smad4, was able to stimulate the promoter activity (Fig. 3*G*). Interestingly, in the −222 to −118 bp region of CYR61 promoter exist two potential Smad-binding elements (SBEs), *i.e.*, SBE1 (GTCTG) at −215 bp and SBE2 (CAGACAGAC) at −205 bp (Fig. 3*E*). While mutation of each single SBE reduced the responsiveness of CYR61 promoter (−222/+15) to TGF-β to different degrees, simultaneous mutation of both SBEs almost abolished TGF-β-stimulated promoter activity (Fig. 3*H*). Chromatin immuno-precipitation (ChIP) examination result showed that TGF-β evidently increased the binding of Smad2/3 to the CYR61 gene promoter (Fig. 3*I*). In addition, a DNA pull-down assay further validated the critical role of SBE1/2 for Smad2/3 to bind to the CYR61 promoter, as mutation of the two SBEs abrogated the protein-DNA interaction (Fig. 3*J*). Together, these results demonstrate that TGF-β-activated Smad2/3 directly bind to the promoter of CYR61, thereby upregulating its transcription.

TGF-β and YAP/TEAD4 signaling coordinately induce CYR61 gene transcription

Given that TGF-β may also transmit its signal *via* non-Smad signaling molecules and that activated Smads usually cooperate with other transcriptional regulators in controlling gene transcription, we ascertained whether other pathways have any effects on TGF-β-induced CYR61 expression by administrating chemical inhibitors. Intriguingly, blockage of either Smad signaling by SB431542 or YAP activity by verteporfin diminished the induction, whereas interference of other pathways was almost without effects (Fig. 4, *A* and *B*).

In fact, CYR61 has been regarded as a classic target gene of the Hippo/YAP pathway (34, 35). This prompted us to test whether TGF-β/Smad signaling might cooperate with the Hippo/YAP pathway to regulate CYR61 gene transcription. The small chemical XMU-MP-1, a kinase inhibitor of MST1/2, was used to shut down the canonical Hippo signaling and allow the activation of YAP and TAZ (36). Intriguingly, while stimulation with either TGF-β or XMU-MP-1 alone increased CYR61 expression to some extent in HCC cells, addition of both led to a robust enhancement (Fig. 4*C*). Blockage of either Smad signaling or YAP activity led to decrease of TGF-β-evoked CYR61 expression, whereas simultaneous inhibition of the two pathways displayed a more potent effect (Fig. 4*D*). Similarly, SB431542 and verteporfin also inhibited CYR61 expression induced by Hippo signaling inactivation (Fig. 4*E*). In support of these observations, depletion of YAP and/or TAZ *via* siRNAs attenuated TGF-β-induced CYR61 expression, and vice versa, Smad2/3/4 were also required for full

ⓈASBMB

*J. Biol. Chem.* (2024) 300(4) 107208 **3**
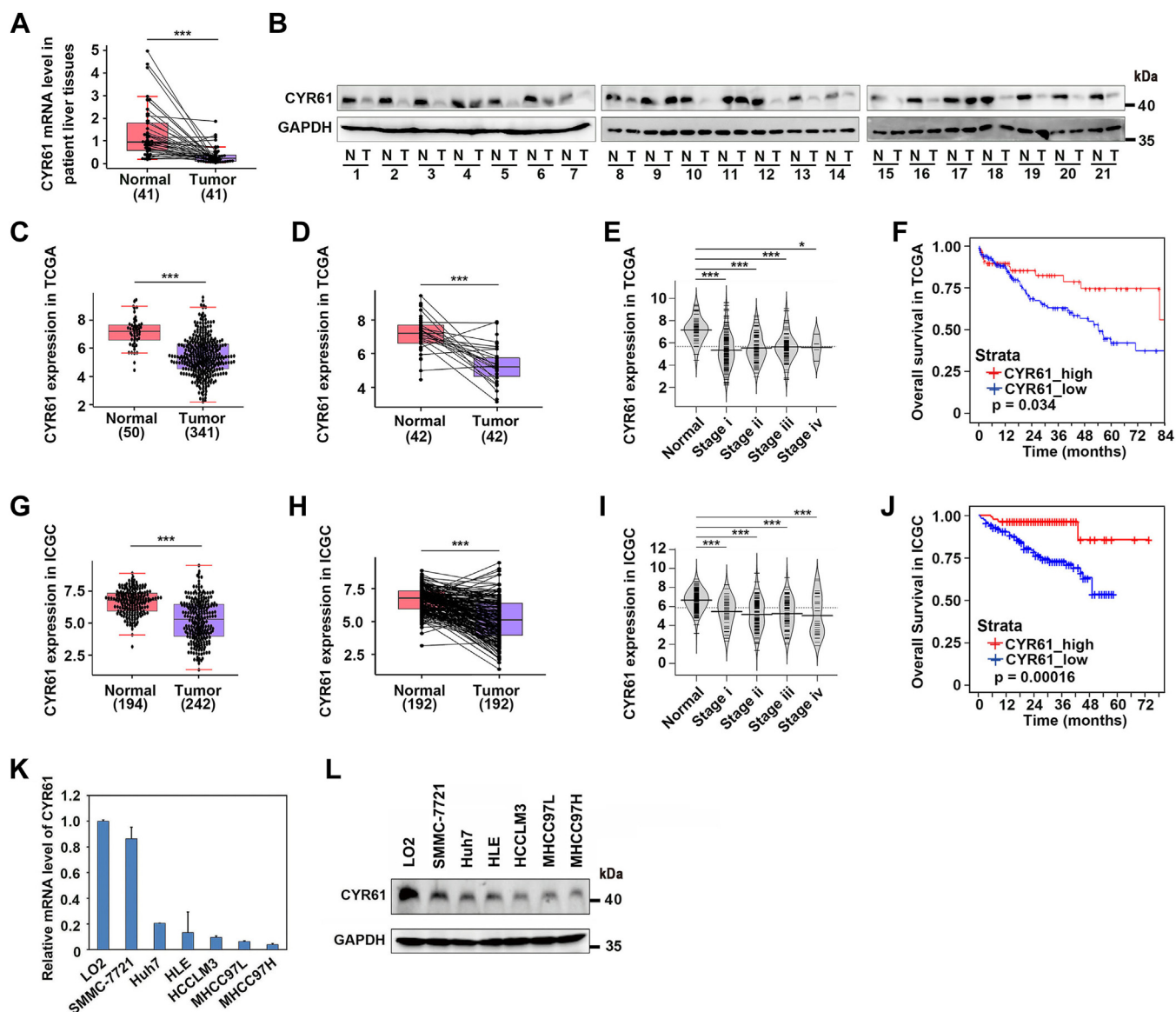
Figure 2. Downregulation of CYR61 correlates with a poor survival rate in human HCC patients. *A* and *B*, paired clinical human HCC tissues and adjacent normal liver tissues were subjected to CYR61 expression analyses by quantitative PCR (n = 41) (*A*) and Western blotting (n = 21) (*B*), respectively. *C*–*E*, comparison of the CYR61 mRNA expression levels between HCC tissues and normal liver tissues (*C*), between paired HCC tissues and normal liver tissues (*D*), or in different TNM stages (*E*) in the TCGA-LIHC database. *G*–*I*, comparison of the CYR61 mRNA expression levels between HCC tissues and normal liver tissues (*G*), between paired HCC tissues and normal liver tissues (*H*), or in different TNM stages (*I*) in the ICGC-LIRI-JP database. *F* and *J*, Kaplan-Meier survival curve analyses illustrating the OS rates of high or low CYR61-expressing HCC patients from TCGA (*F*) and ICGC (*J*) liver cancer databases. *K* and *L*, CYR61 expression was analyzed in different cell lines through quantitative PCR (*L*) and Western blotting (*M*), respectively. *$p < 0.05$, **$p < 0.01$ and ***$p < 0.001$ were calculated using two-tailed student *t* test (*A*, *C*–*E*, and *G*–*I*), and data were shown as mean ± SD. *p*-values for *K* and *L* were calculated using log rank. HCC, hepatocellular carcinoma; LIHC, liver hepatocellular carcinoma; OS, overall survival; TCGA, The Cancer Genome Atlas; TNM, tumor, node, metastasis.

induction of CYR61 by Hippo signaling inhibition (Fig. 4, *F* and *G*). These results suggest that TGF-β signaling and the Hippo pathway can act in concert to regulate the expression of CYR61 in liver cancer cells.

The next question is whether Smad proteins cooperate with YAP/TEADs to directly regulate the promoter activity of CYR61. In accord with previous reports (34, 37), all the CYR61 gene promoter fragments containing the TEAD-responsive element (TRE, 5′-AGCATTCCTG-3′) at −112 bp from the TSS were activated by ectopic YAP (Fig. 5, *A* and *B*). Interestingly, overexpression of YAP and TEAD4 enhanced the activity of CYR61-pro-luciferase reporter (−222/+15) activated

by TGF-β treatment or Smad2/3/4 overexpression (Fig. 5, *C* and *D*). Blocking the activity of either Smads or YAP were able to inhibit TGF-β-mediated activation of CYR61-pro-luciferase reporter (−222/+15) (Fig. 5*E*). Although both the WT YAP or its constitutively active mutant (5SA) could enhance CYR61 gene promoter activity in cooperation with Smad3/4, the TEAD-binding deficient YAP mutants (S94A and 5SA/S94A) were unable to do it, suggesting that both YAP and TEADs are required for Smads-mediated CYR61 expression (Fig. 5*F*). Moreover, disruption of the TEAD-binding site TRE led to a dramatic decrease of the CYR61 promoter responsiveness to TGF-β (Fig. 5*G*). These results reveal that YAP/TEAD
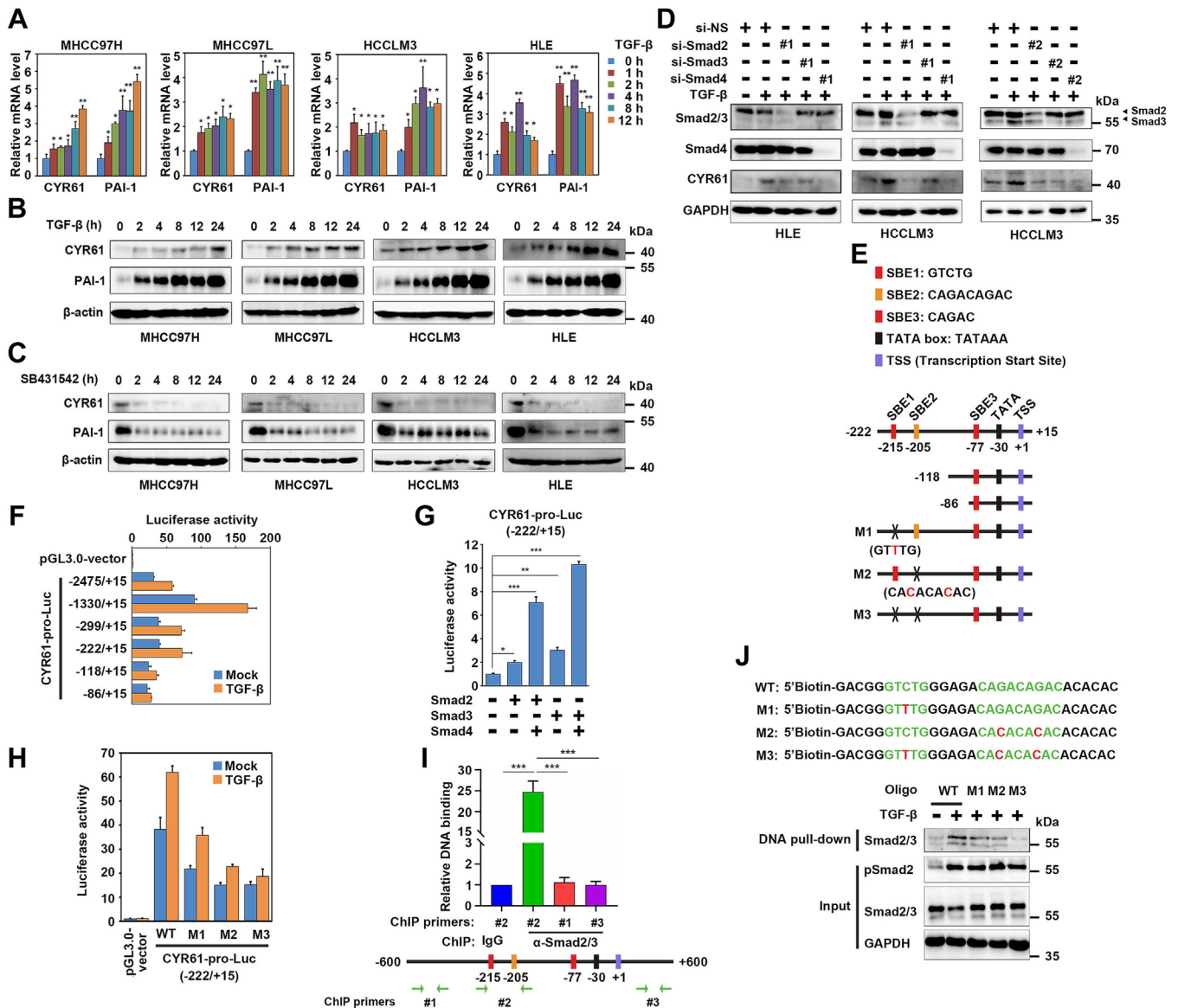
Figure 3. CYR61 is a direct target gene of TGF-β in liver cancer cells. *A*, four different HCC cell lines were treated with or without 2.5 ng/ml of TGF-β1 for the indicated time periods, and then total RNAs were extracted and assessed by quantitative PCR. *B* and *C*, liver cancer cells treated with 2.5 ng/ml of TGF-β1 (*B*) or 5 μM of SB431542 (*C*) were harvested at different time intervals for Western blotting analyses. *D*, HCCLM3 or HLE cells transfected with a control siRNA (NS) or those targeting Smad2/3/4 were treated with 2.5 ng/ml of TGF-β1 for 24 h, followed by western blotting. *E*, schematic diagrams showing different CYR61 promoter regions that were cloned to generate a series of luciferase reporter constructs. Predicted Smad-binding elements (SBEs), TATA box and the transcription start site (TSS) were indicated. *F*, HEK293FT cells transfected with the above CYR61 promoter luciferase reporter constructs (CYR61-pro-luciferase reporters, 200 ng for each) and Renilla-luciferase plasmid (50 ng) were treated with or without 2.5 ng/ml of TGF-β1 for 24 h, followed by luciferase activity measurement. *G*, HEK293FT cells transfected with CYR61-pro-luciferase plasmid (−222/+15, 200 ng), Renilla-luciferase (50 ng) and constructs expressing Smad2, Smad3, or Smad4 for 24 h were subjected to luciferase activity determination. *H*, HEK293FT cells transfected with CYR61-pro-luciferase (−222/+15, with WT or mutated SBE1/2 sites, 200 ng each) were treated with 2.5 ng/ml of TGF-β1 for 24 h before luciferase activity determination. *I*, HCCLM3 cells treated with 2.5 ng/ml of TGF-β1 for 24 h were lysed for ChIP assay using anti-Smad2/3 antibody or the control rabbit IgG, followed by quantitative PCR analysis with a pair of primers as shown in Figure 2I. *J*, HCCLM3 cells treated with 2.5 ng/ml of TGF-β1 for 2 h were lysed for Smad2/3-DNA binding assays using biotin-labeled CYR61 promoter oligos. *p* < 0.05, **p* < 0.01 and ***p* < 0.001 were calculated using two-tailed student *t* test. Data were shown as mean ± SD. ChIP, chromatin immunoprecipitation; HCC, hepatocellular carcinoma; IgG, immunoglobulin G; TGF-β, transforming growth factor-β.

signaling is indispensable for TGF-β-mediated activation of CYR61 gene promoter. On the other hand, we also observed that blocking the activity of either Smads or YAP inhibited YAP-mediated activation of CYR61-pro-luciferase reporter (Fig. 5H). Impairment of Smad-binding sites in the promoter (SBE1/2) also decreased the potency of YAP (Fig. 5I).

Then, we continued to explore the binding of Smad2/3 and YAP/TEAD4 to the CYR61 promoter through ChIP assays. YAP/TEAD activation by XMU-MP-1 treatment enhanced

TGF-β-induced binding of Smad2/3 to the promoter of CYR61 (Fig. 5J), and blockage of the activity of either TGF-β signaling or YAP resulted in reduced Smad2/3 binding (Fig. 5K). On the other hand, TGF-β treatment enhanced the binding of YAP or TEAD4 to CYR61 promoter (Fig. 5, L and M), whereas Smad2/3 knockdown attenuated their bindings (Fig. 5, N and O). Finally, coimmunoprecipitation experiments showed that TGF-β treatment led to association of Smad2/3 with YAP and TEAD4 (Fig. 5, P and Q). In sum, the above results
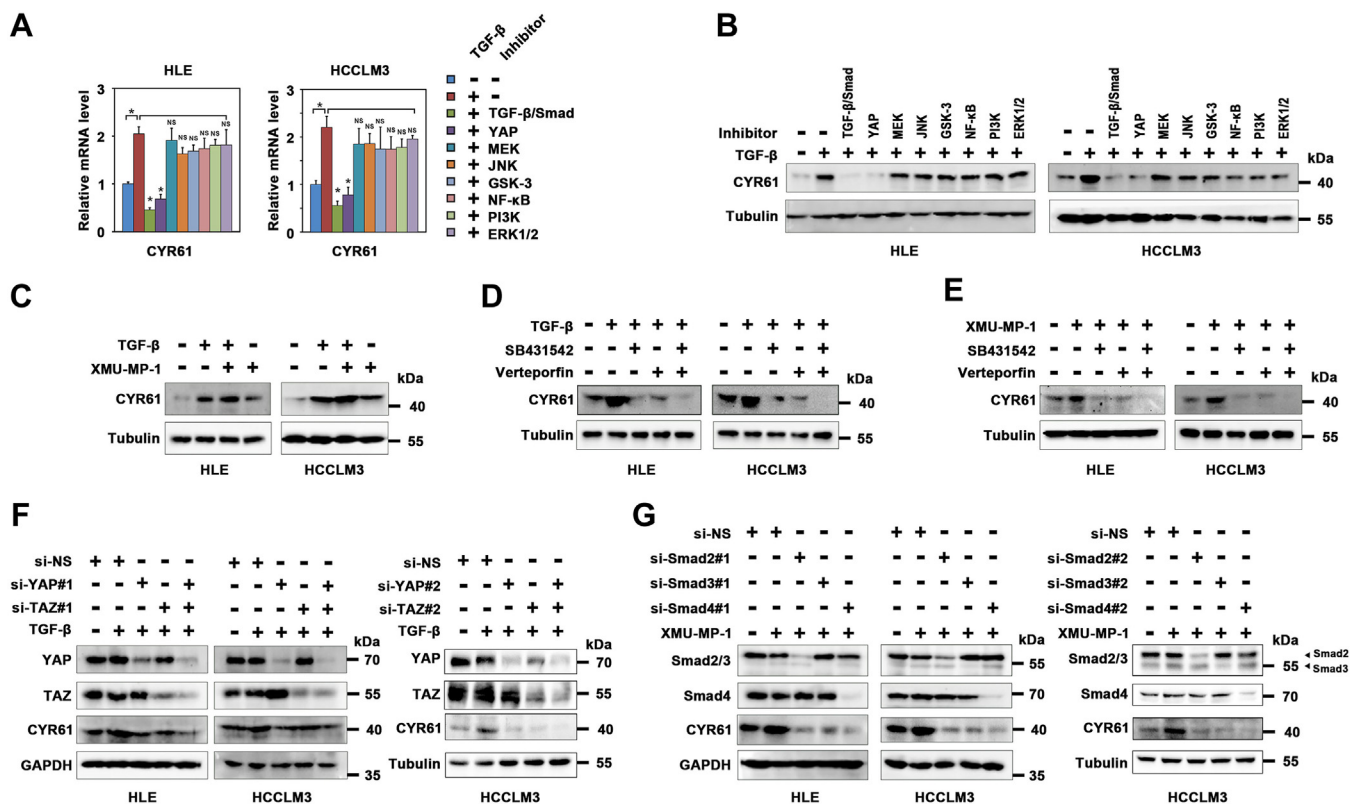
Figure 4. TGF-β and Hippo signaling coordinately regulate CYR61 gene transcription. *A* and *B*, HCCLM3 or HLE cells were treated with 2.5 ng/ml of TGF-β1 in the presence or absence of small chemical inhibitors of different signaling pathways for 24 h, followed by gene expression analyses by quantitative PCR (*A*) or Western blotting (*B*). TGF-β type I receptor inhibitor, SB431542 (5 μM); YAP inhibitor, verteporfin (5 μM); MEK inhibitor, PD0325901 (5 μM); JNK inhibitor, SP600125 (5 μM); GSK-3 inhibitor, SB216763 (5 μM); NF-κB inhibitor, JSH-23 (5 μM); PI3K inhibitor, LY294002 (5 μM); ERK1/2 inhibitor, LY3214996 (5 μM). *C*, HLE or HCCLM3 cells treated with 2.5 ng/ml of TGF-β1 and/or 3 μM of XMU-MP-1 for 24 h were harvested for protein expression detection by Western blotting. *D* and *E*, HLE or HCCLM3 cells were treated with 2.5 ng/ml of TGF-β1 (*D*) or 3 μM of XMU-MP-1 (*E*) for 24 h, in the presence or absence of 5 μM of SB431542 and/or 5 μM of verteporfin. Then cells were analyzed by Western blotting. *F* and *G*, liver cancer cells transfected with siRNAs were treated with or without 2.5 ng/ml of TGF-β1 (*F*) or 3 μM of XMU-MP-1 (*G*) for 24 h before being harvested for Western blotting analyses. TGF-β, transforming growth factor-β.

demonstrate that TGF-β-activated Smads can form a complex with YAP/TEAD4 on the promoter of CYR61, thereby collaboratively stimulating CYR61 gene transcription (Fig. 5*R*).

CYR61 ameliorates TGF-β- and YAP-induced liver cancer progression

As both TGF-β and YAP signaling play a pivotal role in liver cancer progression, we asked whether CYR61 could exert any impacts on the functions of TGF-β or YAP. To answer this, we firstly performed loss-of-function studies of CYR61. As shown in Figure 6, *A* and *B*, compared with a nonspecific control siRNA, three independent CYR61-targeting siRNAs were able to decrease CYR61 expression effectively in HCC cell lines, either at the resting state or upon TGF-β stimulation. Transwell assays revealed that depletion of CYR61 using two of the siRNAs resulted in enhanced migration and invasion of HCCLM3 cells (Fig. 6, *C* and *D*). In addition, treatment of HCCLM3 cancer cells with TGF-β1 and XMU-MP-1, respectively, promoted cancer cell migration and invasion, and these effects were further reinforced by CYR61 silence (Fig. 6, *C* and *D*). In addition, CYR61 knockdown also promoted TGF-β- or YAP-mediated cancer cell growth and proliferation as reflected by 3-[4,5-dimethylthiazol-2-yl]-2,5

diphenyl tetrazolium bromide (MTT) and EdU staining assays (Fig. 6, *E–H*). To validate the functions of CYR61, we established CYR61-or the control vector-expressing stable cell lines by using HLE and HCCLM3 cells (Fig. 7, *A* and *B*). Indeed, ectopic expression of CYR61 inhibited the migration, invasion, growth, and proliferation of HCC cells, either at the basal level or upon stimulation with TGF-β or XMU-MP-1 (Fig. 7, *C–H*).

Next, we established HCCLM3 and HLE stable cell lines that overexpress CYR61 and the constitutively active YAP(5SA), separately or in combination (Fig. 7, *I* and *J*). As shown in Figure 7, *K* and *L*, YAP(5SA) expression promoted the invasion and migration of HCCLM3 cells, while coexpression of CYR61 significantly ameliorated these effects. Moreover, CYR61 also attenuated YAP(5SA)-mediated growth and proliferation of cancer cells (Fig. 7, *M–P*). In addition, the above CYR61-and/or YAP(5SA)-expressing HLE stable cell lines were also used in a xenograft assay. It was found that YAP(5SA) promoted, whereas CYR61 ameliorated the growth of HCC xenograft growth in nude mice (Fig. 7, *Q–S*). The expression of Ki-67 was markedly reduced by CYR61 in the tumor samples (Fig. 7*T*). Together these results reveal that, although transcriptionally upregulated by TGF-β and YAP signaling, CYR61 plays an inhibitory role in TGF-β/YAP-mediated liver cancer progression.
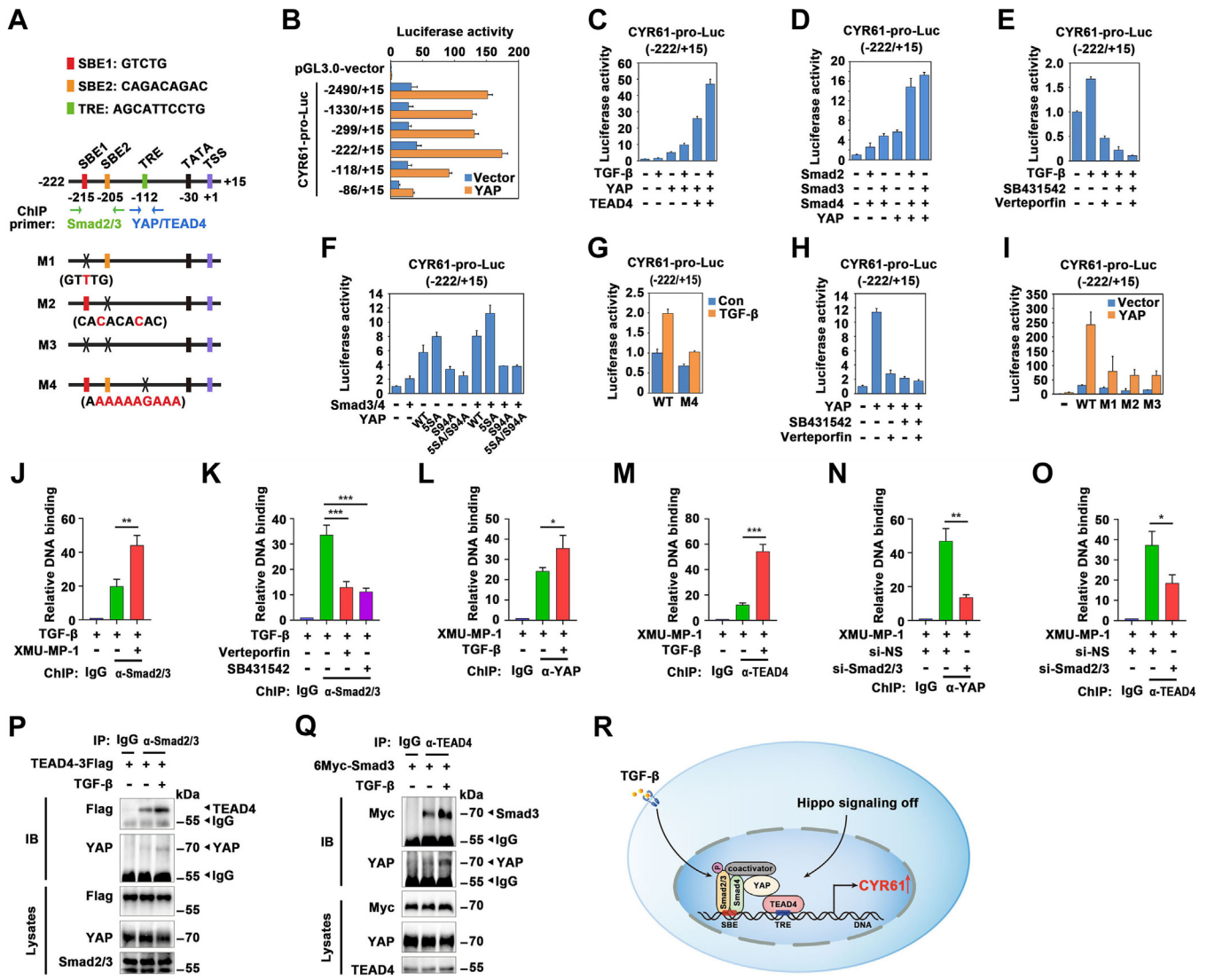
Figure 5. TGF-β-activated Smad proteins cooperate with YAP/TEAD to induce CYR61 gene transcription. *A*, schematic diagrams showing the CYR61 gene promoter regions that were cloned into luciferase-expressing vector. Smad-binding elements (SBEs) and the TEAD-responsive element (TRE) were indicated. *B*, HEK293FT cells transfected with different CYR61-pro-luciferase constructs (200 ng for each), Renilla-luciferase (50 ng), YAP-expressing plasmid (50 ng) or empty vector were harvested for luciferase activity determination. *C*, HEK293FT cells transfected with CYR61-pro-luciferase reporter (−222/+15, 200 ng), Renilla-luciferase (50 ng), YAP- and TEAD4-expressing plasmids (50 ng each) were stimulated with 2.5 ng/ml of TGF-β1 as indicated for 24 h, followed by luciferase activity measurement. *D* and *F*, CYR61-pro-luciferase reporter assays were perfomed in HEK293FT cells by transfecting plasmids expressing Smad2, Smad3, Smad4, and WT YAP or its point mutation derivatives. *E* and *H*, CYR61-pro-luciferase reporter was transfected into HEK293FT cells and activated by treatment with 2.5 ng/ml of TGF-β1 (*E*) or expression of YAP (50 ng) (*H*), with or without stimulation by 5 μM of SB431542 and/or 5 μM of verteporfin for 24 h. *G* and *I*, HEK293FT cells transfected with CYR61-pro-luciferase reporters (−222/+15, WT or mutants) were activated by treatment with 2.5 ng/ml of TGF-β1 for 24 h (*G*) or expression of YAP (50 ng) (*I*), as indicated. *J*–*M*, HCCLM3 cells were treated with 2.5 ng/ml of TGF-β1, 3 μM of XMU-MP-1, 5 μM of SB431542, and 5 μM of verteporfin as indicated for 24 h. Then cells were lysed for ChIP assay using anti-Smad2/3 antibody (*J*–*K*), anti-YAP antibody (*L*) or anti-TEAD4 antibody (*M*) followed by quantitative PCR analyses. *N* and *O*, HCCLM3 cells transfected with siRNAs were treated with 3 μM of XMU-MP-1 before ChIP assays using anti-YAP antibody (*N*), anti-TEAD4 antibody (*O*) or the control IgG. *P*, HCCLM3 cells stably expressing TEAD4-3Flag were treated with or without 2.5 ng/ml of TGF-β1 for 2 h, and then harvested for anti-Smad2/3 immunoprecipitation followed by immunoblotting assays. *Q*, HCCLM3 cells stably expressing TEAD4-3Flag were transfected with a plasmid expressing 6Myc-Smad3 and stimulated with 2.5 ng/ml of TGF-β1 for 2 h. Then immunoprecipitation was performed with anti-TEAD4 antibody. *R*, a schematic diagram showing the cooperation of TGF-β-activated Smads with YAP/TEAD4 in orchestrating the transcription of CYR61 gene in liver cancer cells. *$p < 0.05$, **$p < 0.01$ and ***$p < 0.001$ were calculated using two-tailed student t test. Data were shown as mean ± SD. ChIP, chromatin immunoprecipitation; TGF-β, transforming growth factor-β.

CYR61 elicits an antitumor transcriptional program in liver cancer cells

To seek for the underlying mechanisms by which CYR61 may exerts its tumor-suppressive roles, the CYR61- or vector-expressing HLE cell lines were subjected to transcriptomic sequencing (RNA-Seq). A total of 469 genes were identified to be differentially expressed. DEGs were generated with p-value < 0.05 and a fold change ≥1.4 or ≤0.7, including 119 upregulated genes and 350 downregulated genes, as shown in the heatmap and volcano plots (Fig. 8, *A* and *B*). Importantly, Gene Set Enrichment Analysis (GSEA) analyses indicate that CYR61-regulated genes are negatively correlated with TGF-β and YAP signaling pathways, and also conversely correlated with epithelial-to-mesenchymal transition (EMT) and
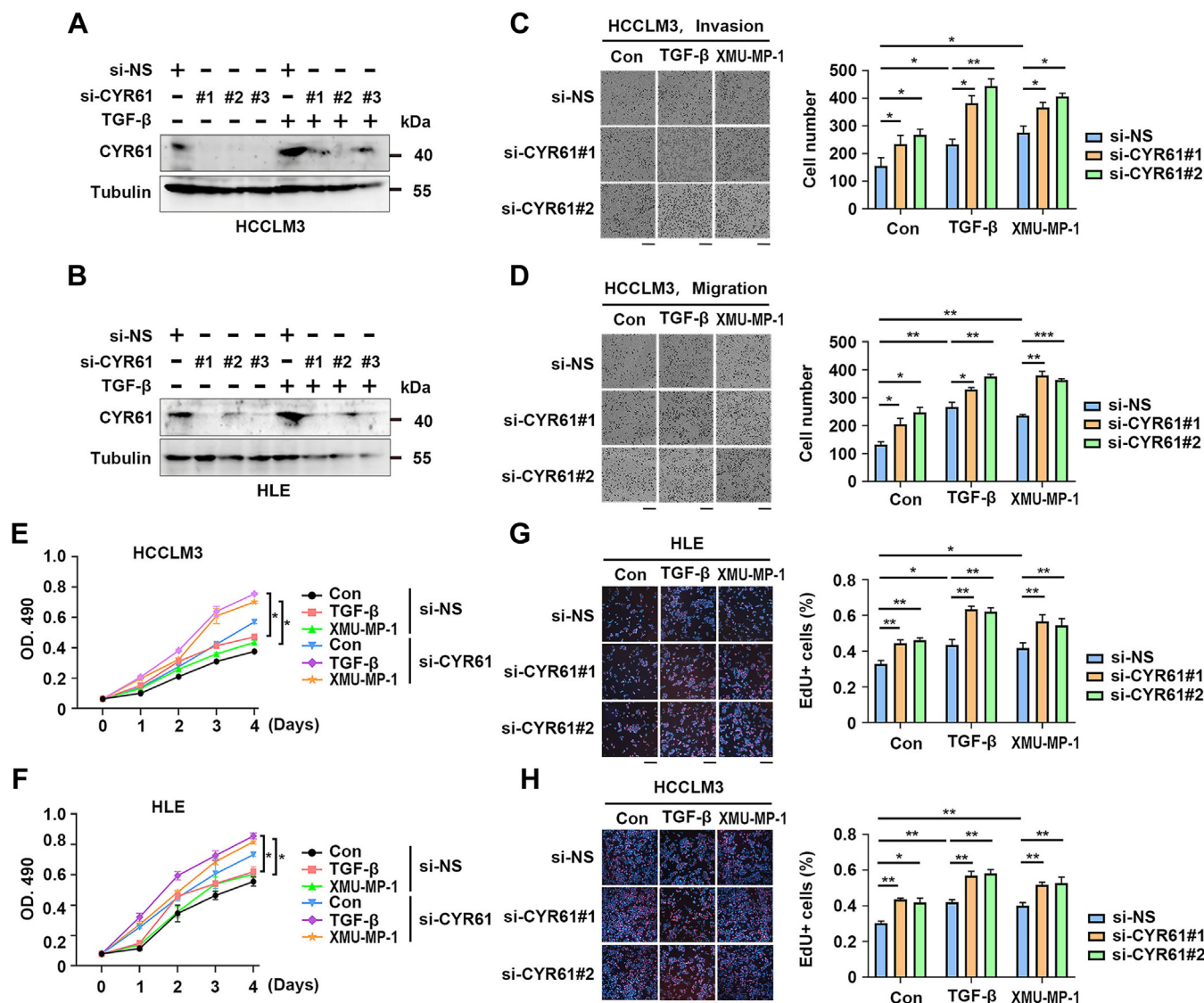
Figure 6. Depletion of CYR61 enhances TGF-β- and YAP activation-induced growth and migration of liver cancer cells. *A* and *B*, HCC cells transfected with a control siRNA (NS) or those targeting CYR61 were treated with TGF-β1 (2.5 ng/ml) for 24 h before being harvested for Western blotting. *C* and *D*, HCCLM3 cells transfected with the control NS or CYR61-specific siRNAs were treated with 2.5 ng/ml of TGF-β1 or 3 μM of XMU-MP-1, followed by matrigel invasion (*C*) or transwell migration (*D*) assays. Invasive and migrated cells were quantified based on three independent experiments. The scale bar represents 100 μm. *E–H*, HCC cells transfected with siRNAs were treated with 2.5 ng/ml of TGF-β1 or 3 μM of XMU-MP-1 for 24 h, followed by MTT assays (*E* and *F*) or EdU staining (*red*) (*G* and *H*). The nuclei were counterstained by DAPI (*blue*) in the EdU staining experiments (*G* and *H*). The scale bar represents 100 μm. DAPI, 4′,6-diamidino-2-phenylindole; HCC, hepatocellular carcinoma; MTT, 3-[4,5-dimethylthiazol-2-yl]-2,5 diphenyl tetrazolium bromide; TGF-β, transforming growth factor-β.

metastasis signature genes, which are already known to be critically involved in cancer cell malignant transformation (Fig. 8, *C–F*). These results are consistent with the fact that CYR61 can impede TGF-β- and YAP-mediated protumor actions in liver cancer.

Discussion

Transcriptional regulation plays a pivotal role in mediating the biological functions of TGF-β or Hippo signaling pathways (2–4, 10–12). To systematically screen for the effectors of TGF-β signaling in HCC, we firstly performed combinatory analyses of our experimental data on TGF-β target genes and public liver cancer databases, including the TCGA and

GEO databases (Fig. 1). This resulted in identification of nine crucial candidate genes, several of which have already been shown to be transcriptional targets of TGF-β and involved in cancer progression, such as PDGFA, FOSB, GADD45B, and CDKN2A (p16INK4A/p14ARF) (38–42). Among them is also found CYR61, which has been documented to either promote or inhibit cancer development dependent on the types of cancer (26, 27, 43). Given its reported protective roles against the development of hepatic inflammation, fibrosis, and liver cancer, CYR61 was selected for further investigation in this study. Indeed, CYR61 is a *bona fide* target gene of TGF-β in liver cancer cells (Fig. 3). Promoter luciferase reporter and ChIP-PCR analyses have identified two important SBEs, *i.e.*, SBE1 (5′-GTCTG-3′) at −215 bp upstream of the TSS of
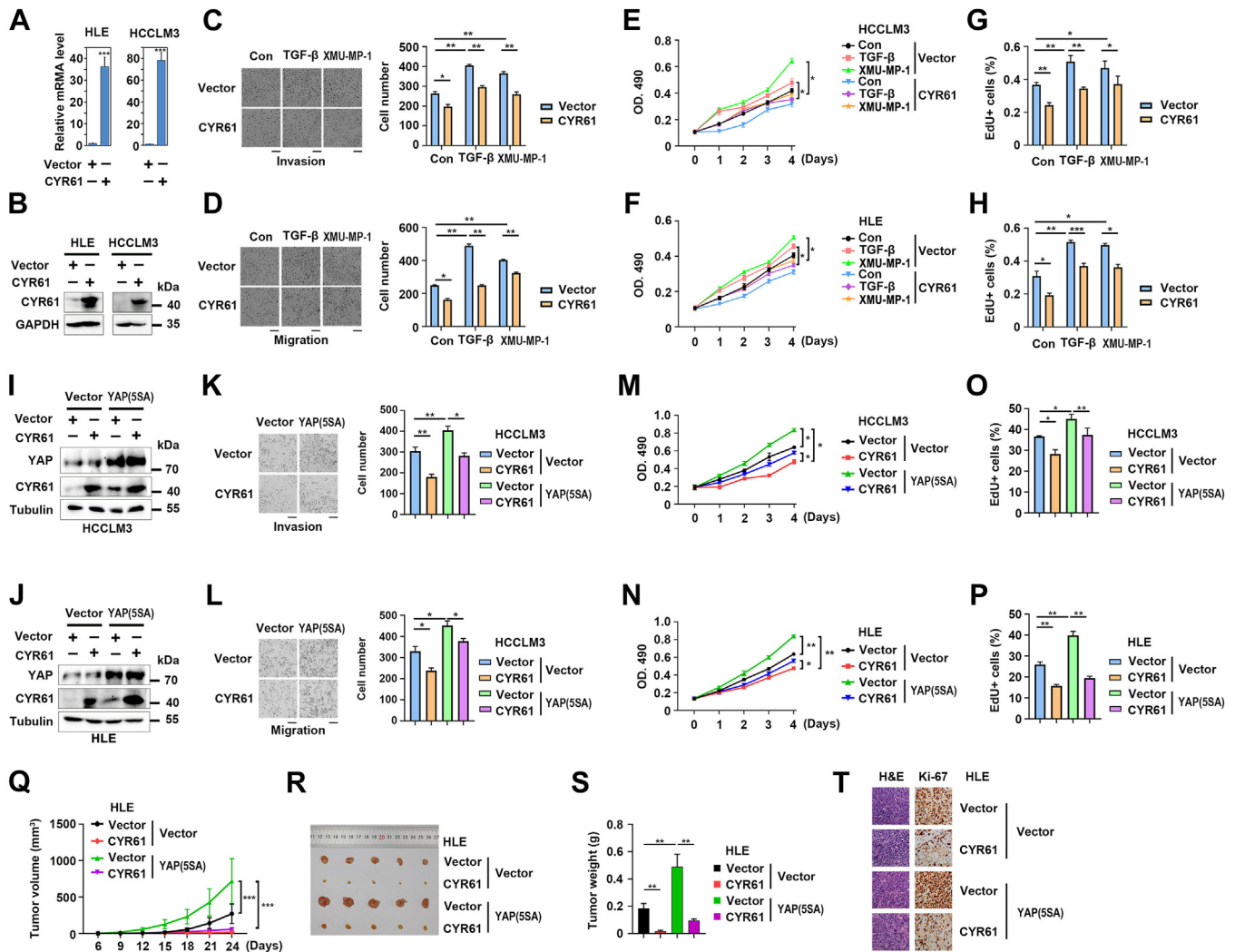
Figure 7. Ectopic CYR61 ameliorates TGF-β- and YAP-induced malignant transformation of liver cancer cells. *A* and *B*, verification of liver cancer cell lines that stably overexpress CYR61 or the control vector by quantitative PCR (*A*) and Western blotting (*B*), respectively. *C* and *D*, HCCLM3 cells stably expressing CYR61 or the control vector were treated with 2.5 ng/ml of TGF-β1 or 3 μM of XMU-MP-1 (3 μM). Then cell growth was monitored by MTT assays at different time intervals. *G* and *H*, CYR61-or vector-expressing cancer cells were treated with 2.5 ng/ml of TGF-β1 or 3 μM of XMU-MP-1 for 24 h, followed by EdU staining (*red*). *I* and *J*, HCC cell lines stably overexpress CYR61 and YAP (5SA), separately or in combination, were verified by Western blotting. *K–P*, HCC cells stably expressing CYR61 and/or YAP(5SA) were subjected to matrigel invasion (*K*), transwell migration (*L*), cell proliferation (*M* and *N*) and EdU staining (*O* and *P*) assays. Experiments were similarly performed as in Figure 5, *C–H*. The scale bar represents 100 μm. *Q–S*, HLE cells stably expressing CYR61 and/or YAP(5SA) were injected into the dorsal abdomen of nude mice. Tumor growth (tumor volume change) in mice was determined at the indicated time (n = 5) (*Q*). Upon mice sacrifice, isolated tumors were assessed in terms of volumes (diameters) (*R*) and weights (*S*), respectively. Data were shown as mean ± SD (n = 5). *T*, representative H&E and Ki67 staining sections from the above xenograft tumor samples. The scale bar represents 200 μm. *$p < 0.05$, **$p < 0.01$ and ***$p < 0.001$ were calculated using two-tailed student *t* test (*A, B, C, D, G, H, K, L, O, P,* and *S*) or two-way ANOVA (*E, F, M, N,* and *Q*). Data were shown as mean ± SD. HCC, hepatocellular carcinoma; MTT, 3-[4,5-dimethylthiazol-2-yl]-2,5 diphenyl tetrazolium bromide; TGF-β, transforming growth factor-β.

CYR61 and SBE2 (5′-CAGACAGAC-3′) at −205 bp. Mutation of the two SBEs abolished the responsiveness of CYR61 promoter to TGF-β and impaired the Smad2/3-DNA binding. Functionally, CYR61 exerts a pivotal tumor suppressor function in liver cancer as detailed below. It is notable that CYR61 can also be transcriptionally induced by TGF-β in some other contexts, mediating the profibrotic functions of TGF-β in the lung and its tumor-promoting effects in osteosarcoma and pancreatic ductal adenocarcinoma (44–46). On the contrary, CYR61 could also alleviate TGF-β-induced fibrosis in the liver or kidney (31, 32, 47). Together, these findings and reports demonstrate that CYR61 acts as an important functional mediator of TGF-β in a context-dependent manner.

Intriguingly, several pieces of evidence in our study demonstrate that the TGF-β and YAP/TEAD signaling pathways cooperate with each other to activate CYR61 gene transcription and regulate liver cancer progression. First, simultaneous stimulation of TGF-β and YAP/TEAD signaling by TGF-β ligand and a Hippo signaling inhibitor XMU-MP-1 led to full induction of CYR61 gene expression, which is higher than that induced by each single pathway. Inhibition or depletion of YAP attenuated TGF-β-induced CYR61 expression, and vice versa, inhibition or knockdown of Smad2/3 also ameliorated CYR61
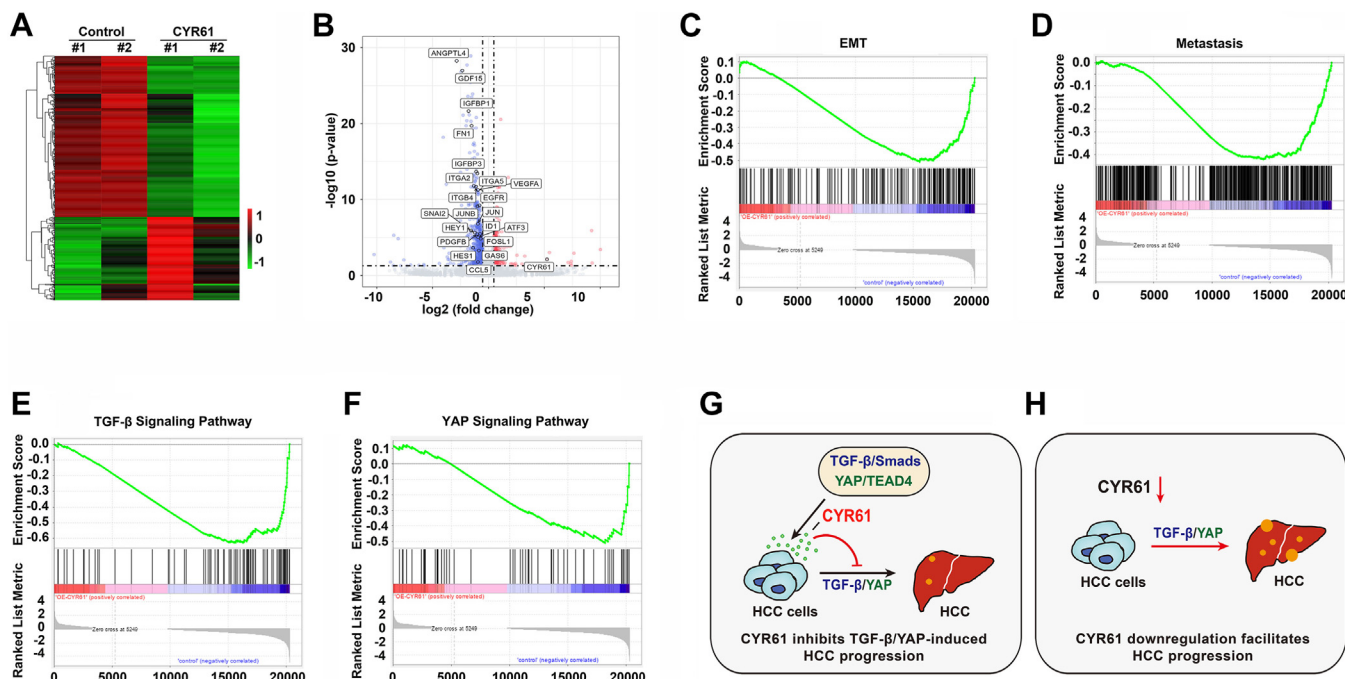
Figure 8. Ectopic CYR61 elicits an antitumor program in liver cancer cells. *A* and *B*, heatmap (*A*) and volcano plot (*B*) classification displaying the 469 genes whose expression levels were significantly altered between CYR61- or the control vector-overexpressing HLE stable cell lines. Some typical tumor-promoting genes were downregulated by CYR61 and illustrated in the volcano plot. *C–F*, GSEA plots depicting enrichments in EMT (*C*), metastasis (*D*), TGF-β signaling (*E*) and YAP pathway (*F*) within CYR61-regulated genes. The *y*-axis represents the enrichment score (ES) and *vertical black lines* on the *x*-axis shows where genes annotated to the respective pathways appear in the ranked list of genes. The colored band represents the ES values (*red* for positive and *blue* for negative). *G* and *H*, schematic diagrams showing the antitumor functions of CYR61 (*G*) and that downregulation of CYR61 facilitates TGF-β/YAP-mediated HCC progression (*H*). EMT, epithelial-to-mesenchymal transition; GSEA, Gene Set Enrichment Analysis; HCC, hepatocellular carcinoma; TGF-β, transforming growth factor-β.

expression mediated by activated YAP (Fig. 4). Second, in the CYR61 promoter region exist two SBEs and a nearby TRE, both of which are required for TGF-β or YAP/TEADs to activate the promoter (Fig. 5). Third, TGF-β-stimulated Smad2/3 and YAP/TEAD4 could associate with their cognate elements in the CYR61 promoter, in a mutually dependent manner (Fig. 5, *B–O*). Fourth, Smad2/3 can form a protein complex with YAP and TEAD4 upon TGF-β signaling activation in liver cancer cells (Fig. 5, *P–R*). Finally, functional experiments indicated that, although transcriptionally induced by TGF-β and YAP, CYR61 exerts a counter-inhibitory function in TGF-β- or YAP-mediated liver cancer malignant progression, thereby generating a negative feedback regulatory loop (Figs 6 and 7). Together, these results are not only consistent with the fact that transcriptional induction of CYR61 is a typical readout of the Hippo/YAP pathway (34, 35), but also demonstrate a novel crosstalk mechanism between TGF-β and Hippo signaling during liver cancer progression. As a matter of fact, several other studies support our notion in this regard. Loss of Lats1/2 or Mob1a/1b in the mice liver has been found to activate YAP/TAZ, which subsequently upregulate TGF-β2 and TGF-β3 that promote liver development or liver cancer progression (48, 49). During liver regeneration, hepatocytes undergo a transient EMT, in which both YAP and TGF-β signaling are activated and necessary (50). To add another piece of evidence, TGF-β has been shown to induce the formation of a Smad2/3-TAZ-p300 complex, which may contribute to myofibroblast differentiation of hepatic stellate cells and stimulate liver metastasis of colorectal cancer cells (51).

Our results have indicated that CYR61 can suppress liver cancer progression by mitigating the tumor-promoting effects of TGF-β and YAP, both in cellular assays and in xenograft mice models (Figs 6 and 7). In addition, transcriptomic studies using RNA sequencing revealed that CYR61-regulated genes are negatively associated with TGF-β signaling, YAP signaling, EMT, and cancer metastasis (Fig. 8). Given that CYR61 has been reported to initiate intracellular signal transduction by binding to membrane integrins (26), such as αVβ3 and αVβ5 in epithelial cells and α6β1 in fibroblastic cells, it would be reasonable to speculate that CYR61 might regulate gene expression and the TGF-β/YAP functions in liver cancer by engaging integrin signaling. Furthermore, in consideration that CYR61 can function in both autocrine and paracrine manners (52), it would be interesting to ask whether cancer cell-derived CYR61 could regulate the communication between cancer cells and other cell types residing in the tumor microenvironment.

Both TGF-β signaling and the Hippo pathway can control the expression of a large array of target genes, some of which may play distinct or even contradictory functions in a certain context or biological process (2, 3, 7, 10, 11, 13). In cancer, both oncogenes and tumor suppressors could be transcriptionally regulated by the two pathways. While balanced expression of these genes is critical for the maintenance of liver homeostasis, dysregulation of the upstream signaling pathways, and/or altered expression of the downstream effectors can impair the balance and have been frequently observed in liver cancer. Indeed, our studies indicated that, when compared with normal liver tissues, liver cancer tissues

exhibit a reduced expression level of CYR61, which is associated with bad clinical outcomes in patients. In sum, our study reveals that the TGF-β and YAP/TEAD4 signaling pathways converge on transcriptional regulation of CYR61, whose downregulation promotes liver cancer progression and may serve as a new diagnostic marker.

Experimental procedures

Mining of DEGs from public cancer databases

The RNA-Seq data of 368 HCC and 50 normal liver tissue samples with clinical information, including 42 paired tumor and normal samples, were downloaded from the TCGA-LIHC database (https://xenabrowser.net/datapages/). Data from TCGA were divided into six cohorts for subsequent bioinformatical analyses (Table S1). In addition, five bulk RNA-Seq datasets (GSE14520, GSE41804, GSE45267, GSE60502, and GSE6764) of HCC and normal liver samples were obtained from the GEO database (http://www.ncbi.nlm.nih.gov/geo/). A total of 650 human HCC and normal liver samples were extracted from the five GEO datasets.

To identify DEGs between HCC and normal tissues, we designed a bioinformatical screening procedure using the above public data (Figs. S1 and S2 and Table S1). GEO datasets were firstly applied for meta-analysis, and DEGs identification from TCGA (cohort 1–4) were conducted with the "edgeR" package (https://www.bioconductor.org/packages/release/bioc/html/edgeR.html). The overlapping DEGs from GEO and TCGA were regarded as candidate genes that may regulate liver cancer development. For validation, the RNA-Seq data of 242 HCC and 192 normal liver tissue samples and related clinical information were also retrieved from the International Cancer Genome Consortium, Liver Cancer-RIKEN, Japan (ICGC-LIRI-JP) database (https://dcc.icgc.org/). Cohorts 5 to 6 from TCGA and cohorts 7 to 8 from ICGC were subjected to gene expression and patient survival analyses (Fig. 2, *C–J* and Table S1).

Cell culture and transfection

Human embryonic kidney epithelial cell line HEK293FT, the hepatocyte cell line LO2, and human HCC cell lines including SMMC-7721, Huh7, MHCC97H, MHCC97L, HCCLM3, and HLE, were all cultured in Dulbecco's minimum essential medium (Solarbio Life sciences) supplemented with 10% fetal bovine serum (Gibco) at 37 °C in a humidified, 5% CO_2 incubator. Cell transfection was conducted with VigoFect (Vigorous Biotechnology) or Lipofectamine 2000 (Invitrogen).

Plasmids, gene silencing, and reagents

Mammalian expression plasmids for Smad2, Smad3, Smad4, TEAD4, and YAP (WT and point mutants including 5SA, S94A, and 5SA/S94A) were fused with HA-, Flag-, or Myc-tags and constructed using the vector pcDNA3.1(+) or pCMV5 (53–55). The full-length complementary DNA of human CYR61 gene was inserted into the pcDNA3.1(+) with a C-terminal Flag tag. The CYR61 gene promoter regions, *i.e.*, the −2475 to +15 bp DNA fragment from the TSS or different

truncations of this region, were cloned into pGL3.0-basic vector to generate CYR61-pro-luciferase constructs.

The nonspecific control siRNA and those targeting human YAP, TAZ, or CYR61 were purchased from RiboBio. siRNAs were transfected with the siTran siRNA Transfection reagent (OriGene). The sequences of siRNAs used in this study were documented in Table S2.

Recombinant human TGF-β1 (CA59) and CYR61 (CB98) peptides were purchased from Novoprotein. Small chemical inhibitors, such as JSH-23 (HY-13982), SB216763 (HY-12012), verteporfin (HY-B0146), SB431542 (HY-10431), PD0325901 (HY-131295), SP600125 (HY-12041), LY3214996 (HY-101494), and LY294002 (HY-10108), were all purchased from MedChemExpress (MCE), while XMU-MP-1 was obtained from AbMole (M9057).

RNA extraction and real-time quantitative PCR

RNA extraction was carried out with TRIzol as previously described (54). Reverse-transcription was performed using the PrimeScript RT Reagent Kit (Toyobo). Quantitative RT-PCR was conducted using the 2× SYBR Green PCR Mastermix (SR1110, Solarbio) in a CFX96 Real-Time System (Bio-Rad). Primers for human genes were collected in Table S3. Gene expression was calculated using the equation RQ = $2^{-\triangle\triangle Ct}$ and normalized to that of GAPDH.

Transcriptome sequencing and data processing

Liver cancer cells were subjected to transcriptome sequencing (RNA-Seq) with the Illumina HiSeq 2000 sequencer in Berry Genomics. Transcriptome construction from RNA-Seq raw data and subsequent analyses were conducted similarly as previously described (54), with updated databases or softwares. Briefly, raw single end reads were trimmed of the first 13 bp from each end and mapped to the human genome (hg38) with TopHat2 (v2.1.1). Gene expression level was estimated and normalized with Cufflinks (v2.2.1) into a fragments per kilobase of transcript per million fragments mapped (FPKM) matrix using default parameters for the annotation GTF file downloaded from GENCODE (v38). DEGs were generated with *p*-value <0.05 and a fold change ≥1.5 or ≤0.6. Gene ontology term and Kyoto Encyclopedia of Genes and Genomes pathway enrichment analyses were performed using WebGestalt (WEB-based Gene SeT AnaLysis Toolkit), with a strict cutoff of *p*-value <0.05. The GSEA software (v4.0.3) was utilized to perform pathway enrichment analyses for CYR61-regulated genes (Fig. 8). To construct the gene set pertaining to the "TGF-β signaling pathway", expression matrices from GSE127763, GSE148795, and GSE222402 were subjected to differential expression analysis using a threshold of |logFC| > 1 and *p* < 0.05. Additional gene sets from the Molecular Signatures Database (MSigDB) were obtained to serve as reference gene sets for other GSEA analyses.

Luciferase reporter assays, immunoprecipitation, immunoblotting, and immunofluorescence

Luciferase reporter assays were carried out as described previously (54). Briefly, cells plated in 24-well plates were

transfected with luciferase reporter construct, Renilla plasmid and other plasmids. Empty vector was used to equalize the total amounts of plasmids in each sample. Luciferase activity was measured by the dual luciferase reporter assay system Berthold LB 960 (Berthold Technologies) according to the manufacture's introduction.

For immunoprecipitation (IP), mammalian cells were plated in 6-well plates or 100 mm dishes one night before transfection. At about 40 h after plasmid transfection, cells were lysed with lysis solution containing 150 mM NaCl, 50 mM Tris–HCl (pH 7.5), 10 mM sodium pyrophosphate, 1 mM sodium orthovanadate dodecahydrate, 0.5% Nonidet P-40 (NP-40), 1 mM EDTA, 10 mM NaF, and protease inhibitors, followed by rotation on a table concentrator at 4 °C for 20 min and centrifugation at 4 °C for 10 min in a microcentrifuge. After being taken by an aliquot for whole protein detection, the supernatants were precleaned by addition of 30 μl protein A sepharose (GE HealthCare) and incubation at 4 °C for 2 h. Then samples were centrifuged gently and the supernatants were transferred to new Eppendorf tubes, and IP was performed by addition of protein A sepharose and appropriate antibodies (2–5 μg), followed by incubation at 4 °C overnight. The immune complex was isolated by gentle centrifugation, washed four times with lysis buffer, analyzed by SDS-PAGE gel and immunoblotting, and finally detected with the enhanced chemiluminescent substrate (Pierce Biotechnology Inc) according to the manufacturer's instructions.

For immunoblotting, cells were lysed with lysis buffer (50 mM Tris–HCl (pH 7.5), 150 mM NaCl, 0.5% NP-40, 1 mM EDTA, 10 mM NaF, 10 mM $Na_4P_2O_7$, and 1 mM Na_3VO_4) containing protease inhibitors. After rotation at 4 °C for 30 min and centrifugation at 13,000 rpm for 15 min at 4 °C, the supernatants were transferred to new Eppendorf tubes, denatured by adding loading buffer (200 mM Tris–HCl (pH 6.8), 8% SDS, 0.4% bromophenol blue, 40% glycerol, and 400 mM DTT) and boiling, and then subjected to SDS-PAGE gel analysis [53]. Normal and cancerous liver tissues were homogenized and lysed with RIPA buffer (Solarbio) containing protease inhibitors, and then protein extraction was similarly carried out as above. For immunoblotting results, the exposure levels of protein bands were analyzed by the Image Pro Plus (https://mediacy.com/image-pro/) software to ensure that the exposures were within the linear range.

In the IP and immunoblotting experiments, anti-TEAD4 (12418-1-AP) and anti-Myc (16286-1-AP) antibodies were bought from Proteintech. Antibodies against α-SMA (250104), COL1A1 (R26615), PAI-1 (381886) and Flag-tag (700002) were purchased from ZEN-Bioscience. Anti-Smad4 (46535S), anti-YAP (12395S), anti-TAZ (4883S) and anti-CYR61 (39382) antibodies were obtained from Cell Signaling Technology. Antibodies recognizing GAPDH (sc-47724), β-actin (sc-8432), and Smad2/3 (sc-133098) were purchased from Santa Cruz Biotechnology.

Chromatin immunoprecipitation

Cancer cells were firstly cross-linked with 1% (v/v) formaldehyde before cell lysis with ChIP lysis buffer that contains 50 mM Tris–HCl pH 8.0, 0.5 mM EDTA, 1% SDS, and protease inhibitors. Then the lysate was sonicated and the chromosomal DNA was broken into fragments of 100 to 800 bp using a Bioruptor Sonicator (Diagenode). After precleaning with bovine serum albumin-blocked protein A sepharose beads, cell lysates were added with appropriate antibodies and incubated at 4 °C overnight. Protein A sepharose beads were subsequently added into each sample and incubated for at 4 °C for 2 h. After washing, beads were eluted with an elution buffer that contains 50 mM $NaHCO_3$ and 1% SDS. Then, samples were digested with the buffer containing 10 mM EDTA, 40 mM Tris–HCl, 1% SDS, and 100 μg/ml proteinase K at 45 °C for 1 h, and reversely cross-linked overnight at 65 °C. Finally, the extracted DNA was analyzed by realtime fluorescence quantitative PCR. The input control was the DNA isolated from cell lysates before precipitation. Primers used for anti-Smad2/3 ChIP assays are as follows: primer pair #1, −411 to −282 bp from the TSS of CYR61 gene, forward 5′-GGCAAAGTTCTGAACTGG-3′ and reverse 5′-GTCAAGAAAACAGTTCGT-3′; primer pair #2, −287 to −143 bp, forward 5′-CTTGACGGGTCTGGGAGACA-3′ and reverse 5′-CCTGGCTCCATTGCACCTT-3′; primer pair #3, +391 to +470 bp, forward 5′-TTTGCGGGTAGCCGTTTC-3′ and reverse 5′-GAAGGCTGCTCCCACCAA-3′. Primers used for anti-YAP and anti-TEAD4 ChIP assays are forward 5′-AAGGTGCAATGGAGCCAG-3′ and reverse 5′-GCGCGTT CCAGAATTCTC-3′, which amplify the −161 bp to −77 bp region in the promoter of CYR61.

DNA pull-down assay

Cancer cells were lysed with DNA-binding buffer that contains 10 mM Hepes (pH 7.5), 150 mM NaCl, 1 mM $MgCl_2$, 0.5 mM EDTA, 0.5 mM DTT, 10% glycerol, and 0.1% NP-40. Then the lysates were incubated with 30 pmol of biotinylated oligonucleotides at 37 °C for 30 min. After addition of streptavidin beads (Sigma-Aldrich), samples were additionally incubated for 15 min. Then, samples were washed thoroughly with DNA binding buffer. The DNA-bound proteins were released by adding protein loading buffer and boiling, and then analyzed by immunoblotting. The biotin-labeled double-stranded oligonucleotides were synthesized by Sangon Biotech.

Lentivirus production and stable cell line establishment

To produce defective lentivirus, HEK293FT cells were transfected with the empty lentivirus vector pL6.3-CMV-GFP-IRES-MCS or the CYR61-expressing derivative (Novobio Scientific), along with the package plasmids pCMVΔ8.9 and VSVG. The culture supernatants were collected at 48 h posttransfection, and the viral particles were concentrated by centrifugation. To establish CYR61-or vector-expressing stable cell lines, cancer cells were infected by lentivirus particles at a multiplicity of infection of 50 pfu per cell. At 48 h post infection, the cells were washed with PBS and complemented with fresh growth medium containing 1 μg/ml of blasticidin. The drug-resistant cells were diluted and dispersed into 96-well plates. Single clones with fluorescence were selected for

expanded culture and subsequently maintained in growth medium containing 0.5 μg/ml of blasticidin.

Transwell assays

Subsequently, 1×10^4 or 1×10^5 cancer cells were seeded in the upper chamber of a transwell system with a pore size of 8.0 μm in the inserts (Corning). After stimulation with recombinant proteins, small chemicals or conditioned medium for 24 h, cells were fixed with 4% formaldehyde fixative solution that was prepared by dissolving paraformaldehyde powder in 1× PBS with a final pH value of 6.9, followed by staining using 1% crystal violet. The membranes were cleaned, air-dried, and photographed under a microscope. Cell number was quantified with the ImageJ (https://imagej.net/software/imagej/) software. Matrigel (BD Biosciences)-coated transwell inserts were utilized in invasion assays, which were subsequently performed similarly as above.

MTT and EdU staining assays

For MTT assay, 1×10^3 cancer cells were seeded in each well of 96-well plates, and each sample was performed in triplicate. After incubation, the plates were added with 20 μl per well of MTT solution (M8180, Solarbio) and incubated at 37 °C for 4 h. After aspiration of the supernatants, cells were incubated with 150 μl of dimethyl sulfoxide (Solarbio) at 37 °C for 30 min. The absorbance was measured at 490 nm in a SpectraMax Paradigm microplate reader (Molecular Devices). For EdU staining, cancer cells were pulse labeled with 50 μM of EdU in Dulbecco's minimum essential medium for 2 h. Then cells were fixed with 4% formaldehyde, permeabilized with 0.5% Triton X-100 in PBS, and stained with the EdU Staining Proliferation Kit (UElandy). Cells were counterstained by Hoechst 33342 (UElandy) for nuclei staining. Images were captured under an Olympus microscope.

Xenograft mice models and analyses

Subsequently, 1×10^7 cancer cells were subcutaneously injected into the bilateral anterior spinal areas of 4-week-old female BALB/c-nu athymic nude mice (SLAC Laboratory Animal Co, five mice per group). The xenograft tumor growth was observed at 6 days post injection, and tumor size was measured every 3 days using a vernier caliper according to the formula V=(L × W^2)/2, where V, L, and W represent the volume, long diameter, and short diameter of tumor, respectively. At 24 days after cell injection, mice were sacrificed and tumors were harvested for immunohistochemistry and Western blotting analyses.

Immunohistochemistry and H&E staining

After fixation in 4% formaldehyde for 24 h, the xenograft tumor blocks were dehydrated, embedded in paraffin, cut into 4 μm-thick slices, deparaffinized with xylene, and rehydrated with alcohol. For immunohistochemistry, endogenous peroxidase in samples was blocked with 0.3% H$_2$O$_2$ for 15 min. After blocking with goat serum for 15 min, slices were incubated overnight with anti-Ki67 antibody (GB121141-50, Servicebio)

overnight at 4 °C, and then with the second antibody, followed by a diaminobenzidine (substrate of peroxidase) revelation and counterstaining with Mayer's hematoxylin. For H&E staining, the rehydrated slices were nuclei stained with hematoxylin for 5 min, differentiated with 0.3% acid alcohol for 1 s, substituted with saturated lithium carbonate for 2 s, and finally stained with eosin. Slices were analyzed under a microscope.

Clinical tumor specimens

Liver cancer tissues and the adjacent normal liver tissues were freshly resected from cancer patients at the Second Affiliated Hospital of Nanchang University. All samples were verified by diagnostic pathology and stored in liquid nitrogen until use.

Ethics statement

Protocols for animal experiments were approved by the Ethical Committee of the Department of Animal Science of Nanchang University and conformed to the guidelines of the National Institutes of Health on the ethical use of animals. The collection and study of clinical liver cancer specimens were also approved by the Ethics Committee of Nanchang University and abided by the Declaration of Helsinki principles. Informed consent was obtained from all participants included in this study.

Statistical analyses

Statistical analyses were performed using R (https://www.r-project.org/, version 4.1.0) and GraphPad Prism (https://www.graphpad.com/, version 8.0). The significance between the means was calculated using two-tailed Student t test as indicated in the figure legends. Each experiment was performed at least in triplicate, and the values were presented as mean ± SD. The Kaplan–Meier method and log-rank test were used for survival analysis of cancer patients.

Data availability

The RNA-Seq raw data and the associated count data that support the findings of this study are openly available in GEO of NCBI (https://www.ncbi.nlm.nih.gov/) under the accession GSE222402 and GSE240760. The cloned human CYR61 gene promoter sequence is documented in GenBank of NCBI under the accession OQ209835.

CYR61 suppresses hepatocellular carcinoma

Y. supervision; S. T. and X. Y. conceptualization; S. T. and X. Y. funding acquisition; C. L., Y. L., W. L., Y. W., X. D., Y. W., and L. Z. software; C. L., Y. L., W. L., Y. W., X. D., Y. W., L. Z., and X. Y. methodology; Chunbo Zhang, Z. L., and Y.-G. C. resources.

Conflict of interest—The authors declare that they have no conflict of interest with the contents of the article.

Abbreviations—The abbreviations used are: ChIP, chromatin immunoprecipitation; DEGs, differentially expressed genes; EMT, epithelial-to-mesenchymal transition; GEO, Gene Expression Omnibus; GO, gene ontology; GSEA, Gene Set Enrichment Analysis; HCC, hepatocellular carcinoma; IP, immunoprecipitation; LIHC, liver hepatocellular carcinoma; MTT, 3-[4,5-dimethylthiazol-2-yl]-2,5 diphenyl tetrazolium bromide; SBE, Smad-binding elements; TCGA, The Cancer Genome Atlas; TGF-β, transforming growth factor-β; TRE, TEAD-responsive element; TSS, transcription start site.

References

1. Vogel, A., Meyer, T., Sapisochin, G., Salem, R., and Saborowski, A. (2022) Hepatocellular carcinoma. *Lancet* **400**, 1345–1362
2. Yimlamai, D., Fowl, B. H., and Camargo, F. D. (2015) Emerging evidence on the role of the Hippo/YAP pathway in liver physiology and cancer. *J. Hepatol.* **63**, 1491–1501
3. Driskill, J. H., and Pan, D. (2021) The hippo pathway in liver homeostasis and Pathophysiology. *Annu. Rev. Pathol.* **16**, 299–322
4. Zhang, S., and Zhou, D. (2019) Role of the transcriptional coactivators YAP/TAZ in liver cancer. *Curr. Opin. Cell Biol.* **61**, 64–71
5. Dituri, F., Mancarella, S., Cigliano, A., Chieti, A., and Giannelli, G. (2019) TGF-Beta as multifaceted orchestrator in HCC progression: signaling, EMT, immune microenvironment, and novel therapeutic perspectives. *Semin. Liver Dis.* **39**, 53–69
6. Gough, N. R., Xiang, X., and Mishra, L. (2021) TGF-Beta signaling in liver, pancreas, and gastrointestinal diseases and cancer. *Gastroenterology* **161**, 434–452
7. Zhang, K., Zhang, M., Luo, Z., Wen, Z., and Yan, X. (2020) The dichotomous role of TGF-beta in controlling liver cancer cell survival and proliferation. *J. Genet. Genomics* **47**, 497–512
8. Fabregat, I., and Caballero-Diaz, D. (2018) Transforming growth factor-beta-induced cell Plasticity in liver fibrosis and hepatocarcinogenesis. *Front. Oncol.* **8**, 357
9. Liu, J., Jin, J., Liang, T., and Feng, X. H. (2022) To Ub or not to Ub: a regulatory question in TGF-beta signaling. *Trends Biochem. Sci.* **47**, 1059–1072
10. David, C. J., and Massague, J. (2018) Contextual determinants of TGFbeta action in development, immunity and cancer. *Nat. Rev. Mol. Cell Biol.* **19**, 419–435
11. Derynck, R., and Budi, E. H. (2019) Specificity, versatility, and control of TGF-beta family signaling. *Sci. Signal.* **12**, eaav5183
12. Russell, J. O., and Camargo, F. D. (2022) Hippo signalling in the liver: role in development, regeneration and disease. *Nat. Rev. Gastroenterol. Hepatol.* **19**, 297–312
13. Misra, J. R., and Irvine, K. D. (2018) The hippo signaling Network and its biological functions. *Annu. Rev. Genet.* **52**, 65–87
14. Franklin, J. M., Wu, Z., and Guan, K. L. (2023) Insights into recent findings and clinical application of YAP and TAZ in cancer. *Nat. Rev. Cancer* **23**, 512–525
15. Moon, H., Ju, H. L., Chung, S. I., Cho, K. J., Eun, J. W., Nam, S. W., *et al.* (2017) Transforming growth factor-beta promotes liver tumorigenesis in mice via up-regulation of Snail. *Gastroenterology* **153**, 1378–1391
16. Bellomo, C., Caja, L., Fabregat, I., Mikulits, W., Kardassis, D., Heldin, C. H., *et al.* (2018) Snail mediates crosstalk between TGFbeta and LXRalpha in hepatocellular carcinoma. *Cell Death Differ.* **25**, 885–903
17. Reichl, P., Dengler, M., van Zijl, F., Huber, H., Fuhrlinger, G., Reichel, C., *et al.* (2015) Axl activates autocrine transforming growth factor-beta signaling in hepatocellular carcinoma. *Hepatology* **61**, 930–941
18. Mazzocca, A., Fransvea, E., Dituri, F., Lupo, L., Antonaci, S., and Giannelli, G. (2010) Down-regulation of connective tissue growth factor by inhibition of transforming growth factor beta blocks the tumor-stroma cross-talk and tumor progression in hepatocellular carcinoma. *Hepatology* **51**, 523–534
19. Xu, M. Z., Chan, S. W., Liu, A. M., Wong, K. F., Fan, S. T., Chen, J., *et al.* (2011) AXL receptor kinase is a mediator of YAP-dependent oncogenic functions in hepatocellular carcinoma. *Oncogene* **30**, 1229–1240
20. Cheng, J. C., Wang, E. Y., Yi, Y., Thakur, A., Tsai, S. H., and Hoodless, P. A. (2018) S1P stimulates proliferation by upregulating CTGF expression through S1PR2-mediated YAP activation. *Mol. Cancer Res.* **16**, 1543–1555
21. Attisano, L., and Wrana, J. L. (2013) Signal integration in TGF-beta, WNT, and Hippo pathways. *F1000prime Rep.* **5**, 17
22. Ben Mimoun, S., and Mauviel, A. (2018) Molecular mechanisms underlying TGF-beta/Hippo signaling crosstalks - role of baso-apical epithelial cell polarity. *Int. J. Biochem. Cell Biol.* **98**, 75–81
23. Hiemer, S. E., Szymaniak, A. D., and Varelas, X. (2014) The transcriptional regulators TAZ and YAP direct transforming growth beta-induced tumorigenic phenotypes in breast cancer cells. *J. Biol. Chem.* **289**, 13461–13474
24. Beyer, T. A., Weiss, A., Khomchuk, Y., Huang, K., Ogunjimi, A. A., Varelas, X., *et al.* (2013) Switch enhancers interpret TGF-beta and Hippo signaling to control cell fate in human embryonic stem cells. *Cell Rep.* **5**, 1611–1624
25. Fujii, M., Toyoda, T., Nakanishi, H., Yatabe, Y., Sato, A., Matsudaira, Y., *et al.* (2012) TGF-beta synergizes with defects in the Hippo pathway to stimulate human malignant mesothelioma growth. *J. Exp. Med.* **209**, 479–494
26. Kim, K. H., Won, J. H., Cheng, N., and Lau, L. F. (2018) The matricellular protein CCN1 in tissue injury repair. *J. Cell Commun. Signal.* **12**, 273–279
27. Yeger, H., and Perbal, B. (2021) The CCN axis in cancer development and progression. *J. Cell Commun. Signal.* **15**, 491–517
28. Feng, P., Wang, B., and Ren, E. C. (2008) Cyr61/CCN1 is a tumor suppressor in human hepatocellular carcinoma and involved in DNA damage response. *Int. J. Biochem. Cell Biol.* **40**, 98–109
29. Chen, C. C., Kim, K. H., and Lau, L. F. (2016) The matricellular protein CCN1 suppresses hepatocarcinogenesis by inhibiting compensatory proliferation. *Oncogene* **35**, 1314–1323
30. Chen, C., Ge, C., Liu, Z., Li, L., Zhao, F., Tian, H., *et al.* (2018) ATF3 inhibits the tumorigenesis and progression of hepatocellular carcinoma cells via upregulation of CYR61 expression. *J. Exp. Clin. Cancer Res.* **37**, 263
31. Kim, K. H., Chen, C. C., Monzon, R. I., and Lau, L. F. (2013) Matricellular protein CCN1 promotes regression of liver fibrosis through induction of cellular senescence in hepatic myofibroblasts. *Mol. Cell. Biol.* **33**, 2078–2090
32. Borkham-Kamphorst, E., Steffen, B. T., Van de Leur, E., Haas, U., Tihaa, L., Friedman, S. L., *et al.* (2016) CCN1/CYR61 overexpression in hepatic stellate cells induces ER stress-related apoptosis. *Cell. Signal.* **28**, 34–42
33. Mooring, M., Fowl, B. H., Lum, S. Z. C., Liu, Y., Yao, K., Softic, S., *et al.* (2020) Hepatocyte stress Increases expression of Yes-associated protein and transcriptional coactivator with PDZ-binding Motif in hepatocytes to promote Parenchymal inflammation and fibrosis. *Hepatology* **71**, 1813–1830
34. Lai, D., Ho, K. C., Hao, Y., and Yang, X. (2011) Taxol resistance in breast cancer cells is mediated by the hippo pathway component TAZ and its downstream transcriptional targets Cyr61 and CTGF. *Cancer Res.* **71**, 2728–2738

35. Xie, L., Song, X., Lin, H., Chen, Z., Li, Q., Guo, T., *et al.* (2019) Aberrant activation of CYR61 enhancers in colorectal cancer development. *J. Exp. Clin. Cancer Res.* **38**, 213

36. Fan, F., He, Z., Kong, L. L., Chen, Q., Yuan, Q., Zhang, S., *et al.* (2016) Pharmacological targeting of kinases MST1 and MST2 augments tissue repair and regeneration. *Sci. Transl. Med.* **8**, 352ra108

37. Zhang, H., Pasolli, H. A., and Fuchs, E. (2011) Yes-associated protein (YAP) transcriptional coactivator functions in balancing growth and differentiation in skin. *Proc. Natl. Acad. Sci. U. S. A.* **108**, 2270–2275

38. van Zijl, F., Mair, M., Csiszar, A., Schneller, D., Zulehner, G., Huber, H., *et al.* (2009) Hepatic tumor-stroma crosstalk guides epithelial to mesenchymal transition at the tumor edge. *Oncogene* **28**, 4022–4033

39. Yoo, J., Ghiassi, M., Jirmanova, L., Balliet, A. G., Hoffman, B., Fornace, A. J., Jr., *et al.* (2003) Transforming growth factor-beta-induced apoptosis is mediated by Smad-dependent expression of GADD45b through p38 activation. *J. Biol. Chem.* **278**, 43001–43007

40. Fischer, A. N., Fuchs, E., Mikula, M., Huber, H., Beug, H., and Mikulits, W. (2007) PDGF essentially links TGF-beta signaling to nuclear beta-catenin accumulation in hepatocellular carcinoma progression. *Oncogene* **26**, 3395–3405

41. Chen, G., Ghosh, P., O'Farrell, T., Munk, R., Rezanka, L. J., Sasaki, C. Y., *et al.* (2012) Transforming growth factor beta1 (TGF-beta1) suppresses growth of B-cell lymphoma cells by p14(ARF)-dependent regulation of mutant p53. *J. Biol. Chem.* **287**, 23184–23195

42. Barrett, C. S., Millena, A. C., and Khan, S. A. (2017) TGF-Beta effects on Prostate cancer cell migration and invasion Require FosB. *Prostate* **77**, 72–81

43. Zhang, C., Li, Z., Hu, K., Ren, Y., Zhang, H., Zhao, Y., *et al.* (2023) The prognostic implications and tumor-suppressive functions of CYR61 in estrogen receptor-positive breast cancer. *Front. Immunol.* **14**, 1308807

44. Kurundkar, A. R., Kurundkar, D., Rangarajan, S., Locy, M. L., Zhou, Y., Liu, R. M., *et al.* (2016) The matricellular protein CCN1 enhances TGF-beta1/SMAD3-dependent profibrotic signaling in fibroblasts and contributes to fibrogenic responses to lung injury. *FASEB J.* **30**, 2135–2150

45. Chen, J., Song, Y., Yang, J., Gong, L., Zhao, P., Zhang, Y., *et al.* (2013) The up-regulation of cysteine-rich protein 61 induced by transforming growth factor beta enhances osteosarcoma cell migration. *Mol. Cell. Biochem.* **384**, 269–277

46. Hesler, R. A., Huang, J. J., Starr, M. D., Treboschi, V. M., Bernanke, A. G., Nixon, A. B., *et al.* (2016) TGF-beta-induced stromal CYR61 promotes resistance to gemcitabine in pancreatic ductal adenocarcinoma through downregulation of the nucleoside transporters hENT1 and hCNT3. *Carcinogenesis* **37**, 1041–1051

47. Liu, H., Zhao, L., Zhang, J., Li, C., Shen, X., Liu, X., *et al.* (2019) Critical role of cysteine-rich protein 61 in mediating the activation of Renal fibroblasts. *Front. Physiol.* **10**, 464

48. Lee, D. H., Park, J. O., Kim, T. S., Kim, S. K., Kim, T. H., Kim, M. C., *et al.* (2016) LATS-YAP/TAZ controls lineage specification by regulating TGFbeta signaling and Hnf4alpha expression during liver development. *Nat. Commun.* **7**, 11961

49. Nishio, M., Sugimachi, K., Goto, H., Wang, J., Morikawa, T., Miyachi, Y., *et al.* (2016) Dysregulated YAP1/TAZ and TGF-beta signaling mediate hepatocarcinogenesis in Mob1a/1b-deficient mice. *Proc. Natl. Acad. Sci. U. S. A.* **113**, E71–E80

50. Oh, S. H., Swiderska-Syn, M., Jewell, M. L., Premont, R. T., and Diehl, A. M. (2018) Liver regeneration requires Yap1-TGFbeta-dependent epithelial-mesenchymal transition in hepatocytes. *J. Hepatol.* **69**, 359–367

51. Wang, Y., Tu, K., Liu, D., Guo, L., Chen, Y., Li, Q., *et al.* (2019) p300 Acetyltransferase is a Cytoplasm-to-nucleus Shuttle for SMAD2/3 and TAZ nuclear Transport in transforming growth factor beta-stimulated hepatic stellate cells. *Hepatology* **70**, 1409–1423

52. Chen, Y., and Du, X. Y. (2007) Functional properties and intracellular signaling of CCN1/Cyr61. *J. Cell. Biochem.* **100**, 1337–1345

53. Yan, X., Liao, H., Cheng, M., Shi, X., Lin, X., Feng, X. H., *et al.* (2016) Smad7 protein Interacts with receptor-regulated Smads (R-Smads) to inhibit transforming growth factor-beta (TGF-beta)/Smad signaling. *J. Biol. Chem.* **291**, 382–392

54. Yan, X., Wu, J., Jiang, Q., Cheng, H., Han, J. J., and Chen, Y. G. (2018) CXXC5 suppresses hepatocellular carcinoma by promoting TGF-beta-induced cell cycle arrest and apoptosis. *J. Mol. Cell Biol.* **10**, 48–59

55. Luo, W., Li, Y., Zeng, Y., Li, Y., Cheng, M., Zhang, C., *et al.* (2023) Tea Domain Transcriptional Factor 4 (TEAD4) mitigates TGF-beta signaling and hepatocellular carcinoma progression independently of YAP. *J. Mol. Cell Biol.* **15**, mjad010